Article

Real-Time PCR Data Processing Shown by the Analysis of Colorectal Specific Candidate Genes, ERCC1, RRM1 and TS in Relation to β2M as Endogenous Control

Melanie Demes [1], Holger Bartsch [1], Stefanie Scheil-Bertram [1], Ralph Mücke [2,3] and Annette Fisseler-Eckhoff [1,*]

[1] Department of Pathology und Cytology, Dr. Horst-Schmidt-Kliniken (HSK), Wiesbaden 65199, Germany; E-Mails: demes@pathologie-wiesbaden.de (M.D.); bartsch@pathologie-wiesbaden.de (H.B.); scheil-bertram@pathologie-wiesbaden.de (S.S.-B.)

[2] Department of Radiotherapy, Lippe Hospital, Lemgo 32657, Germany; E-Mail: ralph.muecke@klinikum-lippe.de

[3] Department of Radiotherapy, St. Josefs-Hospital, Wiesbaden 65189, Germany

* Author to whom correspondence should be addressed; E-Mail: fisseler-eckhoff@pathologie-wiesbaden.de; Tel.: +49-611-43-3419.

Abstract: Currently, quantitative real-time PCR (Q-PCR) of archival formalin-fixed, paraffin embedded (FFPE) tissue is a critical tool for research and is not well established in routine diagnostics. Therefore, continuous improvement in mathematics and statistics associated with interpreting final accurate and reproducible results are fundamental. This project describes and discusses specificity and sensitivity with respect to intra- and inter-assay variances by use of a commercial Human Reference RNA and individual RNA derived from colorectal cancer patients (n = 25). All patients were treated with 5-fluoruracil (5-FU) and a concomitant pelvic radiotherapy (50.4 Gy). Quality assessment of target tissue samples was evaluated by clinicopathological findings and optical density (OD) measurements. We analyzed the steady state messenger RNA (mRNA) expression level of a small panel of cancer relevant genes, excision repair cross-complementing group 1 (*ERCC1*), ribonucleoside-diphosphate reductase subunit M1 (*RRM1*), thymidylate synthase (*TYMS*) and ß-2microglobulin (*ß-2M*) as endogenous control. The mRNA of a Human Reference RNA, tumor and non-neoplastic material was reverse transcribed into its complementary DNA (cDNA). cDNA was amplified based on dual-labeled TaqMan real-time fluorescence measurements. The real-time efficiency and therefore the output

data can be influenced through the kind of calibrator used, the amount and quality of used RNA and by the degree of individual assay variability. Each sample presents an individual amplification curve. Thus, confirmation of primer specificity, one or more invariant endogenous controls, RNA and cDNA quality, as well as real-time PCR amplification efficiencies and linearity calculations from individual slopes or R^2-values must be included in each study.

Keywords: *β2M*; *ERCC1*; Q-PCR-Efficiency; *RRM1*; *TYMS*

1. Introduction

Quantitative real-time polymerase chain reaction (Q-PCR) allows precise and rapid measurements of gene expression, e.g., through dual-labeled probes (ABI's TaqMan assay). This highly sensitive technique has become central to research, for instance, to study the regulation and expression of drug resistance markers in tumor cells or to monitor responses to chemotherapy and to assess the molecular tumor stage, but is not well established routinely [1,2]. The sensitivity requires a great deal of accuracy with regard to experimental design [3]. Assessing the sample quality (e.g., the amount of necrosis or vital tumor cells and RNA quality), especially in formalin-fixed paraffin-embedded (FFPE) samples, is essential for analytical processes which may influence the interpretation of gene expression levels in relation to biological and/or clinical parameters.

The present study describes the experimental design and the data processing obtained by quantitative real-time polymerase chain reaction (Q-PCR) to amplify complementary DNA (cDNA) products, reverse transcribed from mRNA. Direct efforts are also aimed at improving the current methodology with respect to real-time PCR efficiency, which can, for instance, be influenced by cycle conditions, quality and integrity of RNA, kind of endogenous control, efficiency of reverse transcription, kind of calibrator, lab management and unspecific PCR product. The general steps for real-time analysis are explained in detail.

2. Experimental Section

Accurate quantification and quality control (checkpoints) are important to acquire successful and reliable data, as visible in Figure 1.

Human colorectal cancer (CRC) and normal formalin-fixed paraffin-embedded (FFPE) tissue samples were provided by the Institute of Pathology and Cytology of the Dr. Horst Schmidt Kliniken (HSK) in Wiesbaden. 8–14 serial 3 µm-thick paraffin sections were kept at 60 °C for 10 min, deparaffinized (xylol, ethanol) and used for RNA isolation afterwards.

Figure 1. Experimental design (Step 1–3) of the present study, including important checkpoints (→) to provide quality assessment. (NC = Negative control).
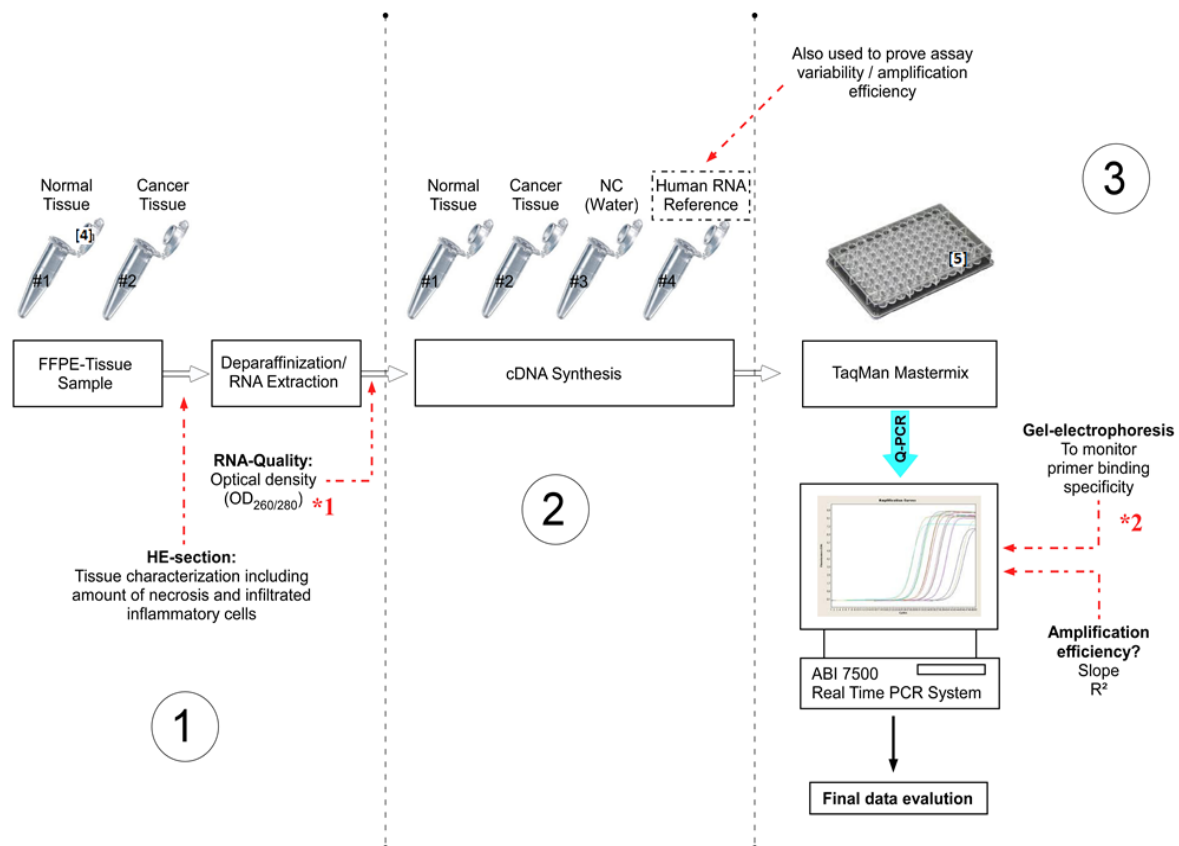
Step 1: FFPE Tissue Sample Characterization, Deparaffinization and RNA Extraction

> *[*1] The RNA quality can be checked by optical density measurements. For RNA integrity the Bioanalyzer 2100 or Experion can be used.*

> *[*2] Alternatively, the amplification specificity can be determined by dissociation curve analysis.*

- Checkpoint: Tissue Sample Characterization

One section per case was HE (hematoxylin & eosin) stained for further characterization of tissue samples regarding the amount of necrosis and inflammatory cells. All tumor samples were diagnosed as low to moderately-differentiated colorectal tumors. All patients were treated with 5-fluoruracil (5-FU) and a total dose of 50.4 Gy. Further patient demographics and clinicopathological findings are depicted in the result part.

The nucleic acid material was isolated from deparaffinized samples manually by using the Recover All Isolation Kit (Ambion) according to the manufacturer´s instructions, with the addition of a 16-h proteinase K lysis step for protein degradation. To avoid DNA contamination interfering with the desired "specific amplification", the RNA samples were treated with RNase-free DNase.

- Checkpoint: Optical Density (A260/280) Measurements of RNA Samples

All nucleic acid concentrations were measured with the NanoPhotometer (Implen). The purity of nucleic acid was assessed by determining the ratio of the absorbance at 260 and 280 nm ($A_{260/280}$) as basic control. An acceptable and realistic nucleic acid quality of FFPE material has an optical density (OD $A_{260/280}$) ranging from 1.8 to 2.1 [6].

The RT efficiency can be affected through salt contaminations, phenols, other alcohols, and inhibitors carried over from RNA isolation process [7]. To assess the RNA integrity by electophoretic separation, the Agilent 2100 Bioanalyzer (Agilent Technologies, USA) or the Experion (Bio-Rad Laboratories, USA) can be used [8]. Undegraded RNA is essential for reliable gene expression analyses. In our study, the RNA integrity was observed by agarose gel electrophoresis. A disadvantage of this method may be the appearance of smears in the case of FFPE-samples. In contrast to miRNA (about ~25 nt (nucleotide) in size) analysis which is growing in importance in oncology, mRNA (up to 10 kb) is more easily degraded by cleavage of RNAes during tissue sampling, purification and storage which also varies significantly between laboratories [9].

Step 2: cDNA Synthesis: Reverse Transcriptase PCR (RT-PCR)

The mRNA strand was first reverse transcribed into its single stranded cDNA (complementary DNA) using the High Capacity cDNA Reverse Transcription Kit (ABI), containing all components necessary for quantitative conversion. The kit includes Random Primers, optimized RT Buffer, dNTP's, RNase Inhibitor and MultiScribe™ MuLV reverse transcriptase.

The cDNA was then further amplified through a quantitative real-time PCR (Q-PCR). For comparative Q-PCR, normal and carcinoma tissue of the same patient were reverse transcribed. Stable "Human RNA-Reference" (Stratagene) was used for assay validation purposes. To confirm the absence of contaminants, a negative control (water control) should be included in the experimental design (Figure 1). A positive control (artificial template with defined concentration) can be used to detect the presence of PCR-inhibitors. To examine the quality and yield of cDNA, two primer pairs of a stable reference gene (~1 kb apart) can be used. The C_T -value of the 5′end primer pair should not exceed that of the 5′end pair by more than 1 C_T [9].

Step 3: Quantitative Real-Time PCR (Q-PCR)

Different technologies exist to investigate the transciptome on RNA level. For instance, the microarray analysis may examine the gene expression of thousands of genes (up to 20,000) in a short time but has a high variability and insufficient sensitivity. Another technique to analyze the mRNA expression level is the RT-PCR by HPLC separation and UV detection or high resolution gel electrophoresis followed by densitometric analysis. In addition, gene quantification can be determined by LightCycler (Roche) or ABI 7500 technologies using "hybridization probes" [9]. The latter one with up to a 96-well standard format was used in this study.

The best-known probe system, which has also been used in the present study, is ABI's TaqMan [7]. The TaqMan gene expression assay is a ready to use 5'-3' *Taq* polymerase assay containing TaqMan® dye-labeled probes (FAM/TAMRA) and desired primers as listed in Table 1.

Table 1. Highly purified salt-free primers for gene targeting (ABI).

Gene	Gene Symbol	Assay	Location	Amplicon-Length
Thymidylate-Synthase	*TYMS*	Hs00426586_m1	Exon 6-7	60 bp
β-2-Microglobulin	*β-2m*	Hs00187842_m1	Exon 1-2	64 bp
Ribonucleotide Reductase M1	*RRM1*	Hs01040705_m1	Exon 8-9	57 bp
Excision Repair Cross-Complementing Repair Gene, Complementation group 1	*ERCC1*	Hs01012158_m1	Exon 3-4	55 bp

In contrast to the available SYBR-green based detection, TaqMan probes detect specific amplification products only.

Probe hydrolysis separates fluorophore and quencher, which results in an increased fluorescence signal which can be measured. This method enables fluorescent monitoring of amplified DNA in real time, at which a threshold amount of amplicon cDNA is produced. The cycle threshold (C_T) value describes the point at which the fluorescence crosses the threshold (Figure 2). According to Pfaffl, the Q-PCR reaction can be divided into four characteristic phases (Figure 2) [7].

Figure 2. Sigmoidal-shaped amplification plot showing increases in fluorescence signal (phase 1–4). Fluorescence signal *versus* cycle number (C_T). *Delta Rn* (= (Rn^+) − (Rn^-)) indicates the magnitude of the signal intensity generated by a given set of PCR conditions. A decreased C_T value (x axis) indicates a higher amount of starting template. The Rn^- value is obtained as a ratio for a PCR without template (the no-template control) and the Rn^+ value is the ratio of FAM fluorescence intensity to the fluorescence intensity of the passive reference dye (ROX) included in the reaction mixture for a PCR with template [7].
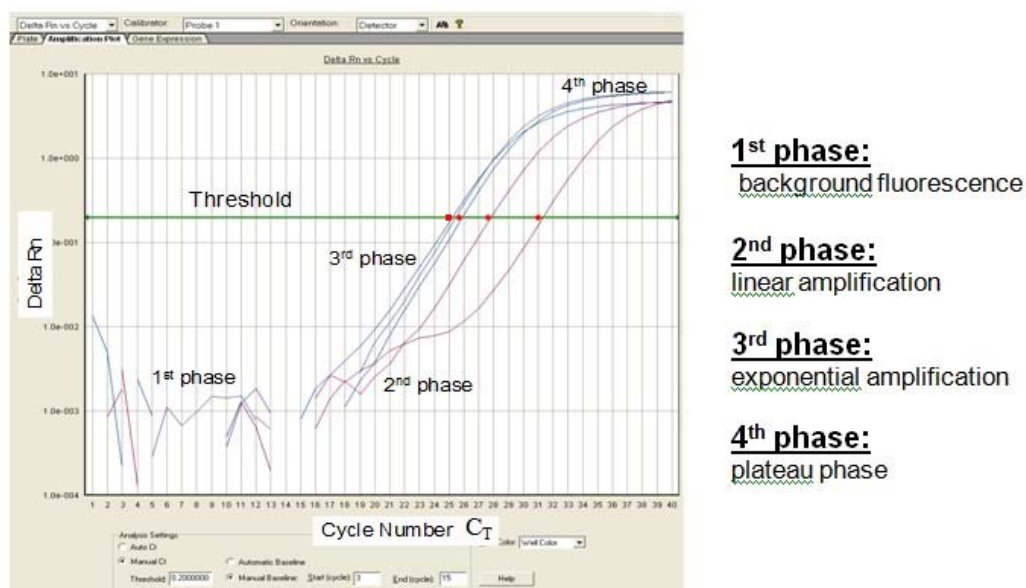
The amount of amplified target is directly proportional to the input amount of target during the exponential phase of PCR amplification.

By using the C_T data, the gene mRNA expression can be explored. The output data of quantitative PCR are shown and discussed in detail later. ß2-*microglobulin (ß2M)*, a component of the MHC

(Major Histocompatibility Complex) class I molecule, was used as endogenous control and normalization factor for the RNA concentration of each sample. Thus, in this experiment, *ß2-microglobulin* gene content should remain constant relative to total nucleic acid. For a comparative gene expression analysis, the specific individual normal tissue of the patient was used as calibrator.

- Checkpoint: Confirmation of Primer Specificity and Amplified PCR End Products

The real-time PCR end product was later documented by 4% ethidium bromide agarose gel staining to ensure proper target amplification, which results in a single band with the desired length (Table 1). Generally, the typical dissociation curve is applied to detect nonspecific amplification in cDNA samples.

- Checkpoint: Test of Endogenous Housekeeping Genes as Adequate Internal Controls

Many classical non-regulated (housekeeping) genes are described. But the biggest problem is that their mRNA expression can be regulated significantly, depending, for instance, on the kind of treatment: in this case, radiochemotherapy (necrosis? inflammation?). Therefore, variances in the target tissue were also investigated between individuals to avoid misinterpretation of biologically relevant information [2,7]. The most common housekeeping genes are, for instance, actins, tubulins, microglobulins and ribosomal RNAs (18S rRNA and 28S rRNA). To investigate the optimal reference gene for normalization of the target gene among all samples, online available programs, *i.e.*, geNorma or Bestkeeper, can be applied.

- Checkpoint: Determination of Inter- and Intra-assay variances as well as Individual Amplification Efficiencies, Including the Dynamic Range

The efficiency of the transcription and Q-PCR was estimated via a standard calibration dilution curve using a conventional RNA Reference (Stratagene) and slope calculation for each assay as B2M, ERCC1, TYMS and RRM1. Slopes between −3.1 and −3.8 are acceptable, giving reaction efficiencies between 90 and 100%. Linear regression analysis indicates the dynamic range. To reduce inter-assay variations, target gene unspecific random-hexamer primers are used to synthesize a cDNA pool (alternatively, octamer- or decamer-primers are available).

If gene-specific PCR primers are designed to produce short products and facilitate multiparallel quantitative analysis, usual criteria such as the GC content (40%, 60%) as well as the length (18 to 25 bases) and Tm (60 ± 1 °C) should be keep in mind [9].

2.1. Final Data Evaluation

Many mathematical and statistical methods exist to evaluate the quantification of mRNA populations. However, the best method to analyze the output data remains an issue of discussion. In the present study, the comparative method ($2^{-\Delta\Delta Ct}$), represented as x-fold expression, was used to compare the mRNA levels of the desired gene in colorectal cancer cells, before and after radiochemotherapeutic treatment, *versus* non-neoplastic cells.

The following figure (Figure 3) illustrates the two widely-applied methodologies for Q-PCR data analysis: relative and absolute quantification. dsDNA melting curve analysis should be performed at the end of the PCR run.

> **Figure 3.** Methodology used to evaluate Q-PCR data. The absolute quantification (1.) relates the PCR signal (cycle number) to the input amount of DNA, using a calibration curve. By use of regression line analysis the amplification efficiency of the whole PCR system can be monitored. Relative quantification (2.) is based on the expression levels of a target gene *versus* the individual normal tissue of the patient (calibrator). Normalization is undertaken by a non-regulated endogenous gene expression, e.g., derived from classical and frequently described housekeeping genes, here *ß2M*.
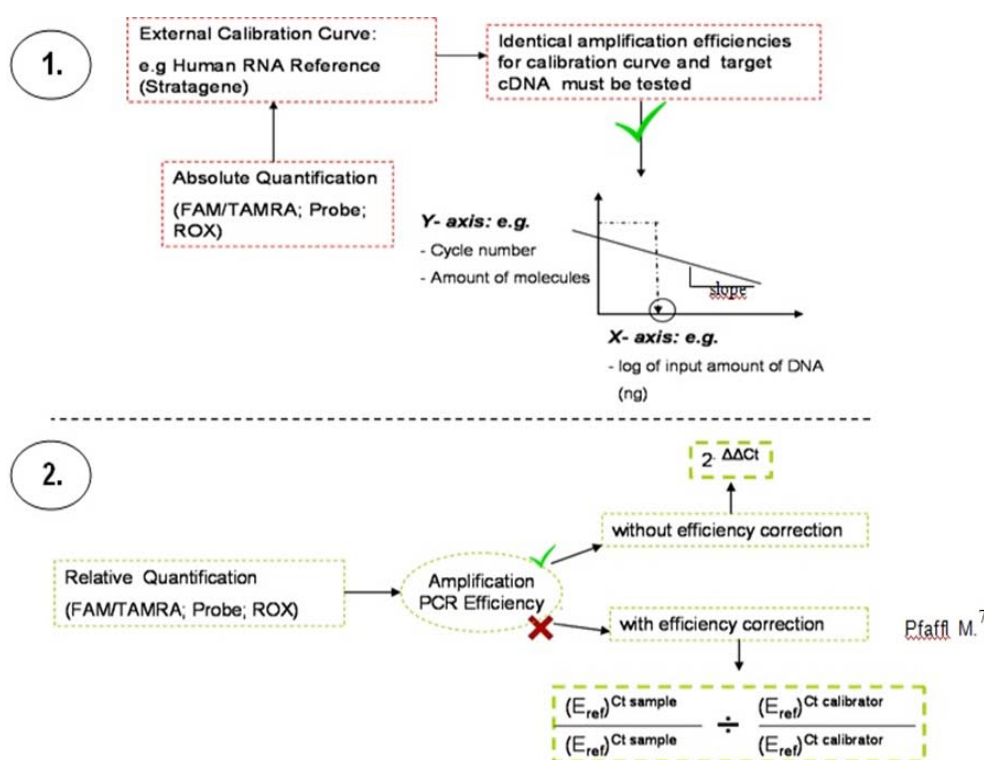
2.2. Statistics and Mathematics

Statistical and mathematical data analysis was done by SPSS 17.0 and JMP 6.0 to determine significant correlations between mRNA expression profiles and patient demographics, including age, sex and regression grading. Significance was set to $P < 0.05$.

3. Experimental Results and Discussion

3.1. Inclusion Criteria and Patient Demographics

The scraped areas of tissue samples used for isolation of the RNA material had to fulfill some inclusion criteria and were characterized in terms of RNA-Quality, presence of necrosis, viable tumor cells and inflammatory cells such as lymphocytes and granulocytes. Thus, the respective sample of the patient had to meet the following criteria to be included in this study:

- Low to moderate amount of lymphocytic and granulocytic infiltration
- Low to moderate amount of necrosis
- RNA quality in an acceptable range of 1.8–2.1 [6]
- High Q-PCR assay linearity (correlation of coefficient; r > 0.99) according to Pfaffl, 2001 [1]
- A good Q-PCR run will have an efficiency ranging from 90%–110% [10]
    - ➔ Q-PCR slopes ranging from −3.1 to −3.6 [10]

Table 2 describes the most important tumor characteristics. The samples were classified as invasive colorectal adenocarcinoma (n = 25) with mostly ulcerated moderately-differentiated tumors. The tumor grading was undertaken according to the American Joint Committee on Cancer (AJCC), pTNM-classifications system and the regression grade as recommended by Dworak [11].

Table 2. Tumor characteristics.

Histological grading (WHO)	
G1 (well differentiated)	1 (4%)
G2 (moderately differentiated)	22 (88%)
G3 (poorly differentiated)	2 (8%)
Tumor stage	
pT1	2 (8%)
pT2	8 (32%)
pT3	15 (60%)
Nodal stage	
pN0	19 (76%)
pN1-2	6 (24%)
Metastases	
pM0	23 (92%)
pM1	2 (8%)
Regression grading (Dworak *et al*. 1997)	
0	1 (4%)
1	5 (20%)
2	9 (36%)
3	10 (40%)

As visible in Table 3, of a series of 25 patients, 13 (52%) samples were from men and 12 (48%) from women. The median age was 67 years (range: 30–84 years).

Table 3. Patient demographics.

Number of Patients	25
Age at diagnosis, years (range)	29 to 84
Median age, years	67
Gender: Female	12 (48%)
Male	13 (52%)

3.2. Histopathology

As mentioned above, tissue characterization is very important to assess the reliability of resultant Q-PCR data and reduce changes in the expression of, e.g., the endogenous control. Tumor tissue and normal tissue at stage of diagnosis and after radiochemotherapeutic treatment were characterized according to morphological appearances (Figure 4).

Figure 4. Hematoxylin and eosin (HE), ×10. Micrographic pictures of normal and tumor colonic tissue illustrating morphologic changes at stage of diagnosis and after neoadjuvant radiochemotherapy. (**A**) Normal structure of a non-tumoral colonic tissue, (Riemann *et al.* 2005), reflecting the typical components of the large intestinal wall of patient number 47 (**B**). (1) Goblet cells, (2) Lamina propia, (3) Crypt of Lieberkühn, (4) Paneth cells, (5) Muscularis mucosae, (6) Blood vessel, (7) Tunica mucosa, (8) Tunica submucosa, (9) Tunica muscularis externa; (**C**) Biopsy of an invasive moderate-grade colorectal adenocarcinoma at stage of diagnosis of patient no. 93. Desmoplastic and cytoplastic effects with partly retained glandular-like structures and a high density of hyperchromatic cells infiltrating the submucosa; (**D**) Resected tumor material of an invasive moderate-grade colorectal adenocarcinoma after neoadjuvant radiochemotherapy of patient no. 93. Scarred fibrotic components with atypical epithelium, desmoplasia and weak lymphocytic infiltration.
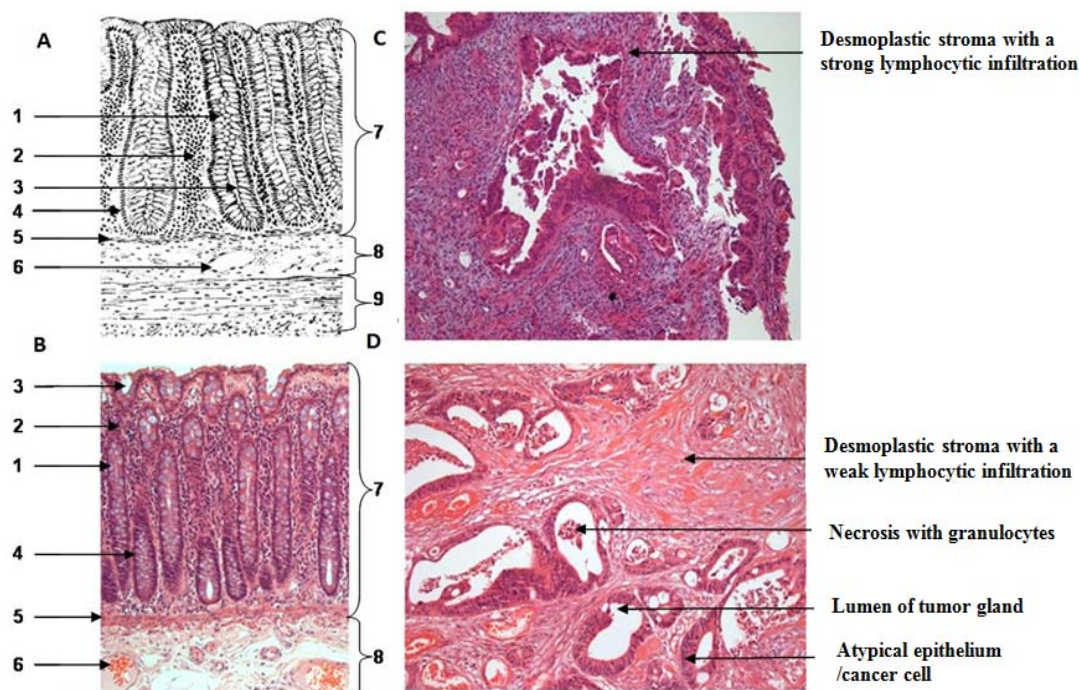

The patients were treated with fluorouracil (5-FU) and a total dose of 50.4 Gy (single dose 1.8 Gy) was applied to the tumor. 5-FU (1000 mg/m^2/d) was administered concomitantly in the 1st (day 1 to 5) and 5th (day 29 to 33) week of radiation as a 120 h-continuous infusion, in two cases partly combined with oxaliplatin and cisplatin, respectively.

Granulocytic and lymphocytic infiltration as well as the amount of viable tumor cells and necrosis are depicted in Figure 5(A,B) and were determined for each HE-stained colonic tumor area used in the

next step for RNA isolation. Most samples contained a large number of viable tumor cells and only a low to moderate amount of necrosis, lymphocytic and granulocytic infiltration before and after neoadjuvant radiochemotherapy. Therefore, the necessary inclusion criteria were met for further analytical steps.

Figure 5. Histomorphological Characterization. (**A**) Samples (n = 50) at stage of diagnosis and (**B**) after neoadjuvant radiochemotherapy, used for further analytical purposes. Most samples contain a large number of viable tumor cells and only a low to moderate percentage of necrosis, lymphocytic and granulocytic infiltrations.
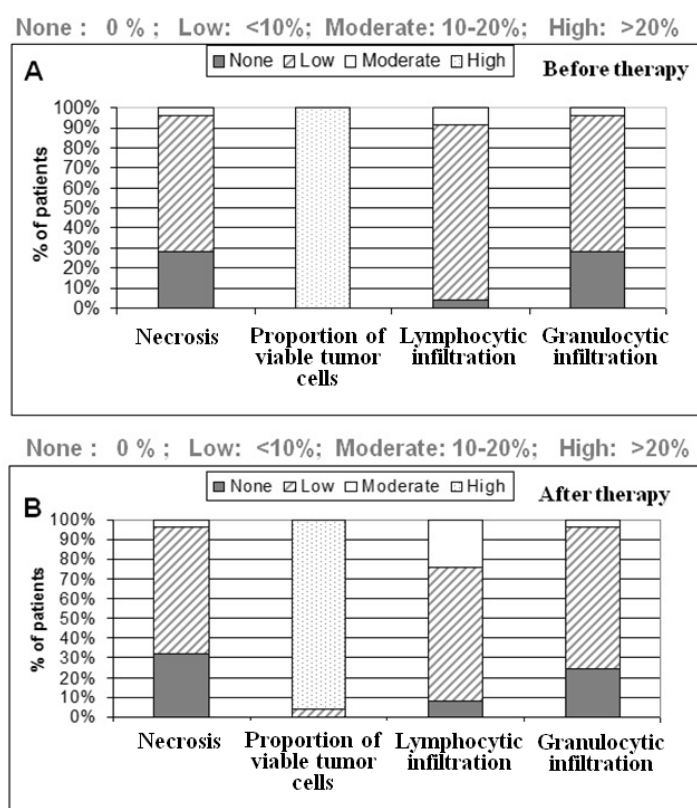
Local and systemic inflammatory responses play an important role in the progression of a variety of common solid tumors. Inflammatory processes result in an overall infiltration of inflammatory cells. These have a high metabolic activity and increased necrosis by, for instance, the production of TNF-α (tumor necrosis factor-α) through e.g., macrophages. This can limit the mRNA expression appraisal. Therefore, extreme care was taken to obtain representative tumor areas with a low percentage of necrosis and only few lymphocytic and granulocytic infiltrations. A large number of tumor cells enhances the chance to detect point mutations.

3.3. Optical Density (A$_{260/280}$) of RNA Samples

Variations in quantity and quality of samples due to partial degradation or the presence of contaminations can influence the data outcome. Thus, it is very important to work under reproducible conditions for every sample.

Table 4 presents the overall purity and thus the quality of all isolated RNA samples collected before and after treatment of 25 patients. As a basic control, the purity of the nucleic acid was determined according to the ratio of the absorbance at 260 nm and 280 nm ($A_{260/280}$), ranging in this study from 1.8 to 2.1. To investigate the RNA, samples can be electrophoretically separated by applications from both Bioanalyzer and Experion.

Table 4. Optical density ($OD_{260/280}$) of nucleic acid including the purchased RNA Reference (Stratagene).

Nucleic acid	$OD_{260/280}$ (mean)	$OD_{260/280}$ (median)	$OD_{260/280}$ (standard deviation)
RNA	1.9	1.8	0.283
RNA Reference (Stratagene)	1.9	1.9	0

All absorbance values obtained were in an acceptable range. Therefore, all samples remained included in this study. The diagrams (Figure 6) also illustrate an overall poorer RNA quality in tumor tissue compared to corresponding normal tissue. The conventional Reference RNA (Stratagene), used to assess the efficiency of the Q-PCR system by the standard dilution curve method, showed the best stable quality even after several repeats, indicated by an $OD_{260/280}$ of 1.9 (Table 4).

Figure 6. RNA purity characterized by optical density ($OD_{260/280}$) measurements. By considering all FFPE samples, the highest purity was obtained in RNA samples of normal individual colonic tissue of the patient as compared to corresponding tumor tissue. * aT = tumor tissue sample before treatment; bT = tumor tissue sample after treatment; bN = normal tissue sample after treatment.
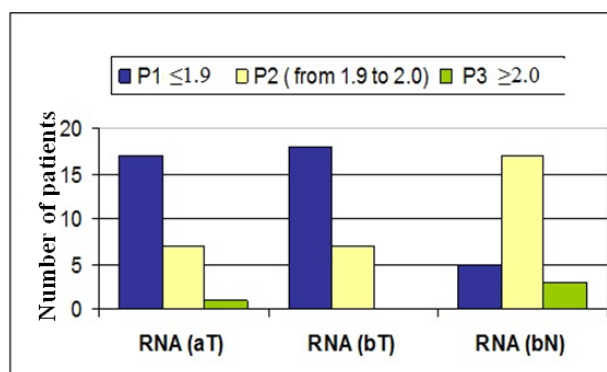
The sensitivity and specificity of the analysis of conventional RNA tumor samples is limited not only by stromal contamination and by heterogeneity within the cancer, but also by the state of the isolated RNA material. RNA is much more labile than DNA, due to high tissue concentrations of endogenous lytic enzymes, and is substantially degraded by formalin fixation and paraffin embedding. Handling and storage of RNA at room temperature can also influence degradation. Extraction of RNA is a long process, often undertaken in the presence of contaminants and ribonucleases that may degrade the nucleic acid. Storage processes can also be a problem, especially for gene analysis. Through the application of shock frozen tissue instead of FFPE samples, as used by some other diagnostic laboratories, can decrease what would otherwise be a rapid degradation or contamination by RNAase of the environment, especially in the case of RNA isolation.

The normal tissue used within this study always came from the closest non-involved area of the patient whose tumor was being studied. A poorer purity of nucleic acid in the colon adenocarcinoma over the normal tissue was demonstrated by optical density measurements.

This was possible due to a high level of enzyme activity in neoplastic tissue above those found in normal tissues from which they originated, and was carried out in accordance with a study performed by Bossmann *et al*. [12]. This study suggested increased degradative enzyme activity may, for instance, act to modify the tumor cell surface, release tumor cells from contact inhibition and permit the epithelial tumor cell to extend through the basement membrane by action of hydrolytic enzymes that could promote the dissolution of some components of the existing basement membrane. This could be a possible explanation for elevated enzyme activity. Therefore, a slight decrease in the optical density for RNA was observed in cancer tissues as compared with normal tissue samples. The quality of a Reference RNA available from Stratagene, which substitutes in some routine diagnostic laboratories the normal individual tissue as calibrator for gene quantification, has the advantage that even after long storage and repeated freezing and thawing the optical density ($OD_{260/280}$ = 1.9) remains stable with no variations in purity by contrast with normal colonic tissue.

3.4. Quantitative Real-Time Polymerase Chain Reaction (Q-PCR): Quality Assurance

3.4.1. Validation of ß2- Microglobulin as an Appropriate Endogenous Control Gene: Inter- Colonic Tissue Variances

Data normalization in real-time RT-PCR is a major step in gene quantification analysis [1,2].

Indeed, it is likely that mRNA levels of the desired housekeeping gene, ß2- microglobulin, vary to such a degree that normalization becomes inaccurate and/or misleading, depending on the experimental conditions and pathohistology of investigated tissue.

Figure 7. Comparison of RNA–ß2- microglobulin gene expression from 25 normal and tumor colon biopsies, respectively.
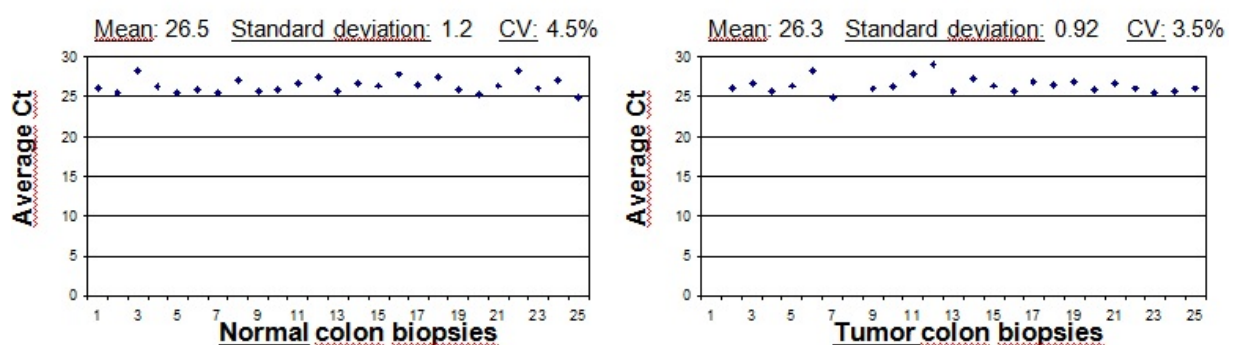
As can be seen in Figure 7, ß2-microglobulin gene expression differs only slightly between different normal and tumor tissue samples and presents a low variability of its expression. Thus, ß2-microglobulin can be used as an internal control gene to obtain reproducible and reliable data. *B2M* solves the problems of variations in template starting amount and operating loading errors [7].

A panel of potential reference genes should be investigated on a representative number of samples to identify the most stable one required for the reliable normalization of RT-PCR data. Additionally, the Normfinder and/or geNorm software can be applied to assess gene expression stability.

3.4.2. Amplicon-Specific Standard Curve Generated by Serial Dilution of a Human RNA Reference (Stratagene)

By the application of the standard curve method, the sensitivity, variability and therefore individual real-time PCR efficiencies were determined for each applied assay used. A standard curve was derived from serial dilutions for each gene investigated (*ERCC1*, *TYMS*, *RRM1* and *B2M*).

The resulting standard curve is generated by plotting the log of target cDNA amount (ng) *versus* the average threshold cycle C_T. As mentioned above, the C_T value is the threshold cycle and presents the detected fluorescence and its geometric increase corresponding to the exponential increase of amplification in each reaction. Linear regression analysis is used to determine the slope and intercept, which respectively correspond to the amplification efficiency and number of amplicon molecules at threshold.

The detection limit, quantification limit and quantification range were determined for every assay, as shown in Figure 8.

Figure 8. (**A1-4**) Standard curve derived from serial dilutions of Reference RNAs (Stratagene) for different assays. (**B1-4**) The equation of the linear regression was determined for each assay of *B2M*, *ERCC1*, *RRM1* and *TYMS*.
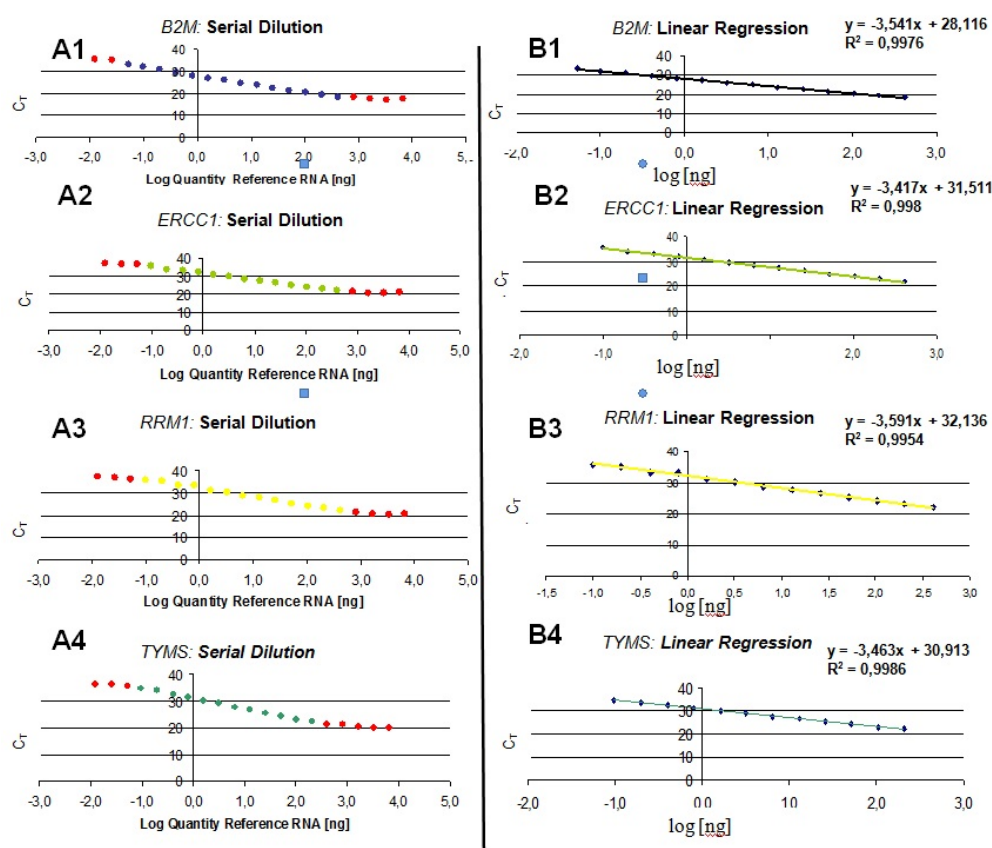
As shown in Figure 8, the real-time PCR provides a large dynamic range. However, very high or very low amounts of RNA used for the following cDNA transcription led to a curtailment and loss of quality indicated by the saturated part of the semi-logarithmic standard curve depicted in Figure 8, (A1-4). To assess quality assurance, an appropriate amount of RNA/cDNA, positioned on the linear regression line, was chosen (Figure 8, B1-4). Thus, an acceptable amount of 25 ng of cDNA was used as input template amount. The standard curves (Figure 8) differ only slightly for the different genes and therefore present a low variability of their expression. For these relatively stable genes, it was possible to obtain a good reproducible standard curve on each plate. Each point represents the average of duplicated determined value and was only used with respect to a low standard deviation (not shown here).

The table below shows the coefficient of determination (R^2 values), standard curve slopes and the efficiency calculated by the instrument. It indicates the proportion of variability and efficiency for each assay.

As visible in Table 5, the slope increases with lower efficiency. This might be because more cycles and thus more amplification is required to reach the fluorescence threshold (Ct) [10].

Table 5. Quality assurance: PCR efficiency.

Gene	R^2 values	Slope	Efficiency (%)
ß2M	0.998	−3.541	91.6
ERCC1	0.998	−3.417	96.2
RMM1	0.995	−3.591	89.9
THYMS	0.999	−3.463	94.4

The efficiency (E) was calculated as follows (ABI, 2008):

$$E = 100 \times (10^{(-1/slope)} - 1) \quad \text{i.e. } E = 100 \times (10^{(-1/-3.463)} - 1) = 94.4$$

According to the literature, efficiency values between 1.6 and 2.1 are realistic [2,10].

The slopes obtained and R^2-values of each standard curve were in an acceptable range according to the literature, which confirm high PCR amplification efficiencies with a low gene expression variability of the endogenous control *ß2M* and the candidate genes *ERCC1*, *RRM1* and *THYMS*. Quality assurance is essential for the maintenance of proficiency in the clinical laboratory. The serial dilution study for each assay demonstrated that the Q-PCR cycle threshold correlated linearly with the quantity of the cDNA in a clinically-relevant dynamic range. 25 ng was then used to meet the linear range and thus ensure quality assurance. In routine diagnostic laboratories it is often the case that only small amounts of tumor cells and therefore RNA are available. Therefore, the usage of lower amounts of RNA material is also an advantage.

The Reference RNA used for the standard curve method is stable with a high efficiency. This RNA can also be applied for determining absolute comparative quantification of target genes by Q-PCR, if the RNA Reference and sample have the same amplification efficiencies

The primer binding specificity was approved by gel-electrophoresis and visualized through ethidium bromide as a basic control (Figure 9). Alternatively, amplification specificities can be determined by dissociation curve analysis.

Figure 9. Confirmation of primer specificity after cDNA-amplification.
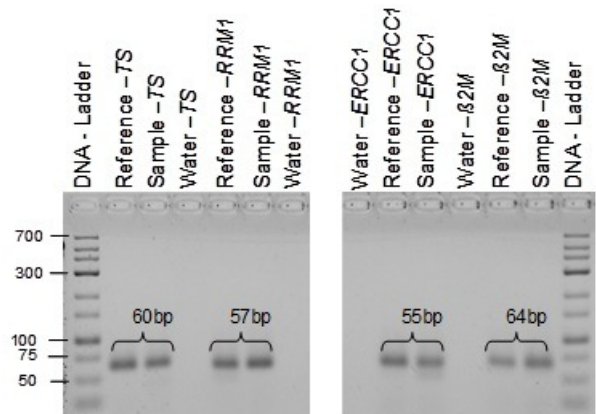
No primer-dimers or amplified contaminated products were generated during 40 real-time amplification cycles. To check for RNA-Integrity, the Agilent 2100 Bioanalyzer or e.g., the Experion can be applied.

2.4.3. Intra- and Inter-Assay Variation: Reproducibility of the Real-Time PCR

The precision and reproducibility of the real-time PCR to further understand the limitations within the system was examined by intra- (replicates in the same PCR run) and inter-assay (replicates in separate kinetic PCR runs) amplification.

As shown in Figure 10, the intra-assay precision was determined in eight repeats of reverse transcription and measured as duplicates. Determination of variation was done in 25 ng transcribed total Human RNA Reference (ABI). The coefficient of variation was determined as depicted in Table 6.

Figure 10. Determination of intra-assay variation in 25ng reverse transcribed total RNA.
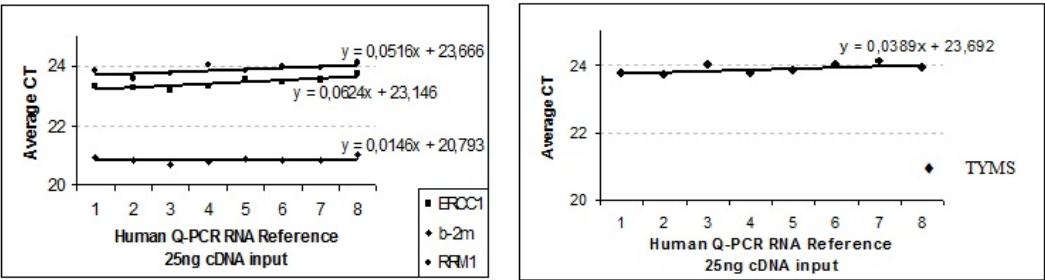

Table 6. Assay variations are based on CP variation and expressed as CP_{mean}, $CP_{standard\ deviation}$ and CV (coefficient of variation).

Assay	CP_{mean}	$CP_{standard\ deviation}$	Intra-Assay Variation (n = 8) CV [%]	Inter-Assay Variation CV [%]
ß-2m	20.87	±0.11	0.5	
ERCC1	23.42	±0.18	0.8	
RRM1	23.9	±0.17	0.7	≤25
TS	23.87	±0.15	0.6	

Inter (CV = <1%) and intra (CV $\leq$ 25%) assay variations are in an acceptable and realistic range according to Pfaffl and Bustin *et al*. [7].

3.4.4. ΔC_T Values of Individual Normal Tissue of the Patient as Calibrator: Assay Variability between Different Individuals.

As shown below (Figure 11), the ΔC_T values were determined for *ERCC1*, *RRM1* and *TYMS* mRNA expression profiles of the respective normal individual tissue collected from 25 patients. The ΔC_T value is the difference between the target gene and endogenous control, described as:

$$\Delta C_T = \text{average } C_T \text{ (target)} - \text{average } C_T \text{ (endogenous control; ß2M)}$$

Example:

$\beta2M_{\text{(Average CT)}}$: nT = 24.860
$ERCC1_{\text{(Average CT)}}$: nT = 29.300
$\Delta C_T = \text{Average } C_T(ERCC1) - \text{Average } C_T(\beta2M)$
$\Delta C_T = \underline{4.44}$

Figure 11. Differences in gene expression are not correlated with age or sex (1 = female; 2 = male). *ERCC1, TYMS and RRM1* assays show the same pattern of variances in gene expression. The *ERCC1* and RRM1 expression profile seems to be more significantly correlated as compared to *TYMS*. *TYMS* is a little bit more variable in its gene expression among different individuals than *ERCC1* and *RRM1*.
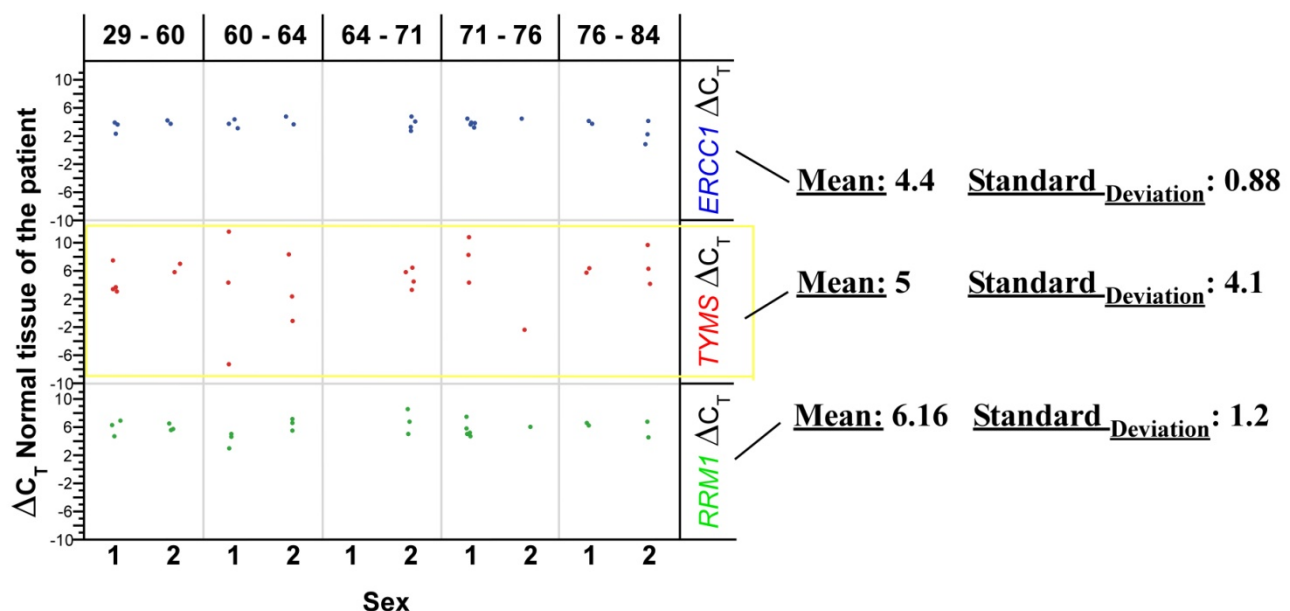
As depicted in Figure 12, no significant correlations between the obtained ΔC_T values, the age (Chi^2-test, $p = 0.358$) and sex (Chi^2-test, $p = 0.274$) were evaluated. *TYMS* indicates a more variable gene expression among different individual patients as compared to *ERCC1* and *RRM1*.

Figure 12. Different relative gene expression profiles for *ERCC1*, *RRM1* and *TYMS* *ERCC1* and *RRM1* show similar expression pattern. It is visible that those patients with an increased *TYMS* expression showed no or only little tumor response (regression grade 0–1) to 5-FU chemotherapy.
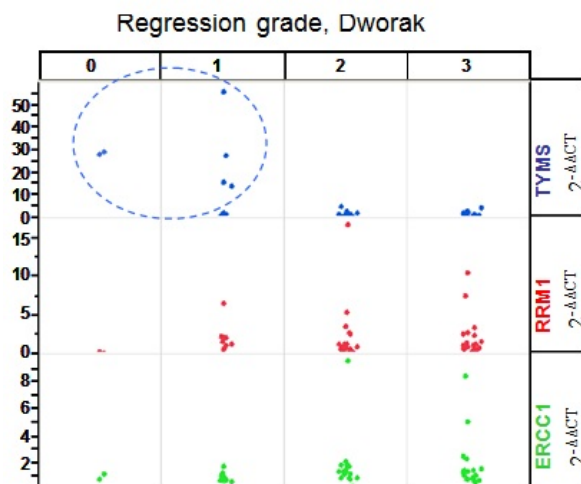
For two patients no fluorescence signals were detected, although the isolated RNA quality was in an acceptable range. One possible explanation might be that the RNA may have contained mutations and therefore the primers could not bind properly and the RNA fragment was not amplified.

Individual changes in gene expression pattern of normal colonic tissue were detected. One can hypothesize that a significant increase in, *i.e.*, *ERCC1* gene expression in normal tissue over the tumor tissue would be the best indicator for successful treatment with platinum-based drugs, because of reduced systemic side effects. Thus, the high activity of repair enzymes (*i.e.*, *ERCC1*) in normal tissue could prevent damage to the DNA and cut out the chemotherapeutic agent rapidly before inducing apoptosis. However, a decreased expression of this repair gene and therefore enzyme in tumor tissue would also be a benefit for the patient. In that case the chemotherapeutic agent can bind and damage the nucleic acid and initiate apoptosis without being cut out directly. Thus, the RNA expression in the normal individual may in addition be used as a predictive value of the effect and outcome of chemotherapeutic drugs.

In this study, the normal colonic tissue of the patient was used as calibrator.

It was established that the quality of the isolated RNA from different samples varied only slightly. Nevertheless, this variation could have an influence on the resulting measured C_T values. Therefore, a stable Reference RNA such as the one available from Stratagene has found its application in some other routine diagnostic laboratories.

However, does this RNA Reference really substitute the individual normal RNA isolated from the colonic tissue of the respective patient where the tumor was also found?

In order to use one Reference RNA (obtained from RNA isolated from different cell culture cells) suitable for all tumor samples investigated, it must be assumed that there is no individual expression level variation of the investigated RNA species between different patients. Because this assumption is difficult to prove, normal tissue from the investigated patients was used.

As normal tissue samples are not always available in all cases in which tumor tissue was obtained, the application of a standard Reference RNA would be an alternative. It should be emphasized that tumor tissue and no single isolated cells were utilized in this study. Therefore, the normal tissue was used as calibrator because otherwise it is difficult to attribute all of the elevated activity to the actual neoplastic cell because some normal cells may be included in the tumor mass.

3.5. $2^{-\Delta\Delta CT}$ Comparative Gene Expression of Individual Tumor Tissue of Each Investigated Patient

The relative gene expression was determined by using the $2^{-\Delta\Delta CT}$ comparative method. All data were normalized to *β2-microglobulin* (*β2M*) mRNA content.

Comparative RNA expression analysis in tumor *versus* normal cells (calibrator) was performed as follows:

Tumor tissue: $\Delta C_T = C_T \text{ (target)} - C_T \text{ (\textit{β2M})}$

Normal tissue: $\Delta C_T = C_T \text{ (target)} - C_T \text{ (\textit{β2M})}$

$\Delta\Delta C_T = \Delta C_T \text{(tumor tissue)} - \Delta C_T \text{(normal tissue)}$

Ratio = $2^{-\Delta\Delta CT}$

Example:

Tumor tissue: $\Delta C_T = 29.304 - 25.211 = \underline{4.09}$

Normal tissue: $\Delta C_T = 29.300 - 24.860 = \underline{4.44}$

$\Delta\Delta C_T = \underline{4.09} - \underline{4.44} = -0.35$

Ratio = $2^{-(-0.35)} = 1.27$

The ΔC_T value was calculated by respectively subtracting the average Ct value of the *β2M* RNA from the average C_T value of the normal tissue and of the tumor tissue. The $\Delta\Delta C_T$ value was calculated by subtracting the ΔC_T value for the normal cells from the ΔC_T value of the tumor cells [13]. Fold of enrichment values was determined according to the ratio $2^{-\Delta\Delta CT}$ (see example).

A correlation between the regression grade and the expression level of *TYMS* was found (Figure 13), including in one female patient who died from this cancer, who had a very high *TYMS* expression level and showed no tumor response to 5-FU radiochemotherapy.

Figure 13. One factor analysis of *TYMS* according to the regression grade (after Dworak) [11]. The t-test also reveals a significant correlation between *TYMS* and the grade of regression by clear separated cycles.
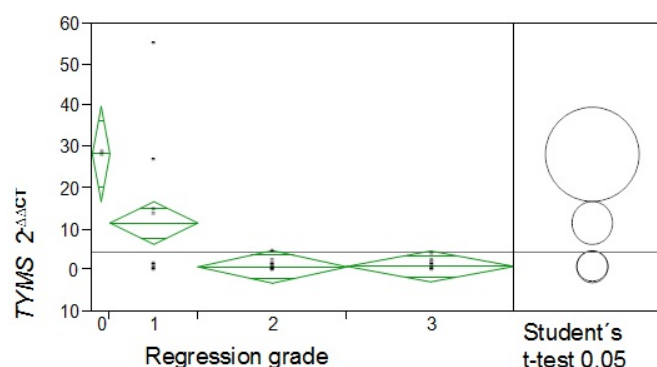
The correlation between *TYMS* and the regression grade was also revealed by the application of further statistical tests such as the t-test as shown in Figure 13.

The interrelation between the different assays was also determined by the Chi^2-test as listed below:

ERCC1 ⟷ *RRM1 = p = 0.001*
ERCC1 ⟷ TYMS = p = 0.30
RRM1 ⟷ TYMS = p = 0.241

Therefore, a correlation between the RNA expression of *ERCC1* and *RRM1* in tumor tissue was statistically supported.

The endogenous control gene allows the gene expression profile of the target gene to be normalized to the amount of input RNA or cDNA. It corrects for variation in possible RNA degradation, differences in sample handling, variation in reverse-transcription efficiency, presence of inhibitors in the RNA sample and RNA content or differences in sample handling. As described in the results section, the comparative method (ratio $\mathbf{2^{-\Delta\Delta CT}}$) was used, including *β2-microglobulin* (*β2M*) as endogenous control and the normal tissue as calibrator [14].

When considering the gene expression pattern, no correlations with sex or age of any patient were detected (Table 7).

Table 7. Correlation between the relative quantification ($2^{-\Delta\Delta CT}$) of each gene target (*ERCC1*, *RRM1* and *TYMS*), the age, sex and regression grade status of all samples statistically evaluated by the application of the Chi^2-test. A statistically significant correlation between *TYMS* and the regression grade was revealed.

Target (RQ)	Age	Sex	Regression grade (after Dworak)[11]
ERCC1	p = 0.4910	p = 0.2179	p = 0.4279
RRM1	p = 0.4765	p = 0.7017	p = 0.1731
TYMS	p = 0.3927	p = 0.1609	p = 0.0221

5-FU targets folate metabolism through the inhibition of thymidylate synthase. It was obvious that all patients with high *TYMS* expression levels showed no or only low response to 5-FU. This observation agrees with the literature which states that the *TYMS* expression is linked to cellular sensitivity or resistance to the drug [15,16]. Other studies found that patients suffering from metastatic cancer with amplified *TYMS* genes have a shorter median survival than those without amplification [17]. As already mentioned, one patient with metastases and *TYMS* amplification showed resistance to 5-FU and died of colorectal cancer within a short period of time.

4. Conclusions

Real-time is mainly used for research purposes and is a well-established methodology.

The workflow of Q-PCR analysis includes several important steps, crucial for successful experimentation, exhibiting high precision, robustness and reliability.

Q-PCR data analyses differ significantly in their performance and especially in pre-PCR steps and quality assurance procedures between different laboratories. There is a need for greater standardization

to make the final result of quantitative expression analysis more comparable between laboratories worldwide (beginning with the usage of isolation kits and ending with final data evaluation).

The quality of tissue samples must therefore also be closely monitored through detailed histopathological tissue characterization and RNA quality tests which should be reported to classify the resultant final data of the respective publication.

Additionally, several potential endogenous controls should be investigated on a representative number of samples to identify the most stable one required for the reliable normalization of RT-PCR data.

PCR-amplification efficiency and primer-specificity have a major impact on the fluorescence history and accuracy of the calculated expression pattern and should be monitored.

Sample characterization, tissue variations and PCR/Q-PCR efficiencies must be carried out prior to any calculations to determine the final experimental design and kind of quantification methods. If needed, efficiency-corrected quantification corrections should be included. Complete and biologically relevant analysis of gene expression requires additional information, especially that derived from immunohistochemistry and biochemical assays.

In the present study, gene expression of *TYMS* in tumor tissue was significantly higher in those patients with resistance to 5-FU chemotherapy. This was also observed in other studies.

ERCC1 and *RRM1* presented a similar expression pattern. One could hypothesize that there might be a correlation between the increased activity of DNA repair (ERCC1) enzyme and the enzyme (RRM1) essential for the production of deoxyribonucleotides. A further detect study with larger CRC series should be analyzed and compared to immunohistological examinations in order to definitely establish clinical relevance.

References

1. Pfaffl, M.W. A new mathematical model for relative quantification in real-time RT-PCR. *Nucleic Acids Res.* **2001**, *29*, e45.
2. Bustin, S.A. Quantification of mRNA using real-time reverse transcription PCR (RT-PCR): Trends and problems. *J. Mol. Endocrinol.* **2002**, *29*, 23–29.
3. Walker, C.G.; Meier, S.; Mitchell, M.D.; Roche, J.R.; Littlejohn, M. Evaluation of real-time PCR endogenous control genes for analysis of gene expression in bovine endometrium. *BMC Mol. Biol.* **2009**, doi: 10.1186/1471-2199-10-100.
4. Thomas Scientific. Eppendorf Lobind Microcentrifuge Tubes. Available online: http://www.thomassci.com/Supplies/Centrifuge-Tubes/_/Eppendorf-LoBind-Microcentrifuge-Tubes/ (accessed on 10 October 2011).
5. Science Fair. Microplates 96 Well. Available online: http://www.thesciencefair.com/Merchant2/merchant.mvc?Screen=PROD&Product_Code=5467-6&Category_Code=MICCHEM (accessed on 10 October 2011).
6. Ayubi, T. *RNA Quality Control. Biomedical Genomics*; 2007. Available online: http://www.biomedicalgenomics.org/RNA_quality_control.html (accessed on 2 June 2011).
7. Pfaffl, M.W. Quantification strategies in real-time PCR. In *A-Z of Quantitative PCR*; Bustin, S.A., Ed.; International University Line (IUL): La Jolla, CA, USA, 2004; Chapter 3, pp. 87–112.

8. Fleige, S.; Pfaffl, M.W. RNA integrity and the effect on the real-time qRT-PCR performance. *Mol. Aspects Med.* **2006**, *27*, 126–139.

9. Pfaffl, M.W. *Livestock Transcriptomics: Quantitative mRNA Analytics in Molecular Endocrinology and Physiology*; 2003. Available online: http://www.gene-quantification.de/habilitation.html (accessed on 15 October 2011).

10. Cottrell, M.; Waidner, L. *qPCR Protocol I: ABI Instrument*; Applied Biosystems: Carlsbad, CA, USA, 2008.

11. Dworak, O.; Keilholz, L.; Hoffmann, A. Pathological features of rectal cancer after preoperative radiochemotherapy. *Int. J. Colorectal Dis.* **1997**, *12*, 19–23.

12. Bossmann, H.B.; Hall, T.C. Enzyme activity in invasive tumors of human breast and colon. *Proc. Natl. Acad. Sci. USA* **1974**, *71*, 1833–1837.

13. Finis, K.; Sültmann, H.; Ruschhaupt, M.; Buness, A.; Helmchen, B.; Ruprecht, K.; Gross, M.-L.; Fink, B.; Schirmacher, P.; Poustka, A. Analysis of pigmented villonodular synovitis with genome-wide complementary DNA microarray and tissue array technology reveals insight into potential novel therapeutic approaches. *Arthritis Rheum.* **2006**, *54*, 1009–1019.

14. Livak, K.J.; Schmittgen, T.D. Analysis of relative gene expression data using real time quantification PCR and the $2^{-\Delta\Delta CT}$ method. *Methods* **2001**, *25*, 402–408.

15. Gusella, M.; Bolzonella, C.; Crepaldi, G.; Ferrazzi, E.; Padrini, R. A novel G/C single-nucleotide polymorphism in the double 28-bp repeat thymidylate synthase allele. *Pharmacogenomics J.* **2006**, *6*, 421–424.

16. Lenz, H.J.; Leichman, C.G.; Danenberg, K.D.; Daneberg, P.V.; Groshen, S.; Cohen, H.; Laine, L.; Crookes, P.; Silberman, H.; Baranda, J. Thymidylate synthase mRNA level in adenocarcinoma of the stomach. A predictor for primary tumor response and overall survival. *J. Clin. Oncol.* **2003**, *14*, 176–182, 199.

17. Wang, T.L.; Diaz, L.A.; Romans, K.; Bardelli, A.; Saha, S.; Galizia, G.; Choti, M.; Donehower, R.; Parmigiani, G.; Shih, I.-M. Digital karyotyping identifies thymidylate synthase amplification as a mechanism of resistance to 5-fluorouracil in metastatic colorectal cancer patients. *Proc. Natl. Acad. Sci. USA* **2004**, *101*, 3089–3094.

18. Shea, P.Y.; Shing, S.T.; Polly H.M.; Tsz, S.C.; Peter, K.C.; Wilina, W.L. Use of dual TaqMan probes to increase the sensitivity of 1-step quantitative reverse transcription-PCR: Application to the detection of SARS coronavirus. *Am. Assoc. Clin. Chem.* **2005**, *51*, 1885–1888.